

Award Number:

W81XWH-08-1-0289

TITLE:

Characterizing the relationship between blast exposure and mild TBI with dynamic modeling and testing in a new mouse model

PRINCIPAL INVESTIGATOR:

Candace L. Floyd, Ph.D.

W. Steve Shepard, Jr. Ph.D.

CONTRACTING ORGANIZATION:

The University of Alabama at Birmingham
Birmingham, AL 35249

REPORT DATE:

July 2010

TYPE OF REPORT:

Annual

PREPARED FOR: U.S. Army Medical Research and Materiel Command
Fort Detrick, Maryland 21702-5012

DISTRIBUTION STATEMENT:

√ Approved for public release; distribution unlimited

The views, opinions and/or findings contained in this report are those of the author(s) and should not be construed as an official Department of the Army position, policy or decision unless so designated by other documentation.

REPORT DOCUMENTATION PAGE

Form Approved
OMB No. 0704-0188

Public reporting burden for this collection of information is estimated to average 1 hour per response, including the time for reviewing instructions, searching existing data sources, gathering and maintaining the data needed, and completing and reviewing this collection of information. Send comments regarding this burden estimate or any other aspect of this collection of information, including suggestions for reducing this burden to Department of Defense, Washington Headquarters Services, Directorate for Information Operations and Reports (0704-0188), 1215 Jefferson Davis Highway, Suite 1204, Arlington, VA 22202-4302. Respondents should be aware that notwithstanding any other provision of law, no person shall be subject to any penalty for failing to comply with a collection of information if it does not display a currently valid OMB control number. **PLEASE DO NOT RETURN YOUR FORM TO THE ABOVE ADDRESS.**

1. REPORT DATE (DD-MM-YYYY) 31-07-2010		2. REPORT TYPE Annual		3. DATES COVERED (From - To) 1 JUL 2009 - 30 JUN 2010	
4. TITLE AND SUBTITLE Characterizing the relationship between blast exposure and Mild TBI with dynamic modeling and testing in a new mouse model				5a. CONTRACT NUMBER	
				5b. GRANT NUMBER W81XWH-08-1-0289	
				5c. PROGRAM ELEMENT NUMBER	
6. AUTHOR(S) Candace L. Floyd, Ph.D W. Steve Shepard, Jr. Ph.D. Email: cfloyd@uab.edu				5d. PROJECT NUMBER	
				5e. TASK NUMBER	
				5f. WORK UNIT NUMBER	
7. PERFORMING ORGANIZATION NAME(S) AND ADDRESS(ES) University of Alabama at Birmingham 546 Spain Rehabilitation Center 1717 6 th Ave. S. Birmingham, AL 35249-7330				8. PERFORMING ORGANIZATION REPORT NUMBER	
9. SPONSORING / MONITORING AGENCY NAME(S) AND ADDRESS(ES) U.S. Army Medical Research and Materiel Command Fort Detrick, MD 21702-5012				10. SPONSOR/MONITOR'S ACRONYM(S)	
				11. SPONSOR/MONITOR'S REPORT NUMBER(S)	
12. DISTRIBUTION / AVAILABILITY STATEMENT Approved for public release: distribution unlimited					
13. SUPPLEMENTARY NOTES					
14. ABSTRACT The purpose of this research is to determine through analytical modeling and animal-based experiments the blast-level threshold for mild traumatic brain injury in humans. We have cataloged brain material properties and determined axon bundle geometry. Basic axon geometry has been determined for a finite element (FE) model and modified geometry has also been developed. Blast pressure profiles for small IED and other blast scenarios have been determined from literature reviews. Preliminary models have been constructed. In a tandem effort, laboratory-based animal experiments are being conducted to determine the impact forces that induce single or repetitive mTBI in mice. A 0.196J impact to the closed mouse skull caused a transient loss of consciousness, which suggests that a mild TBI occurred. Two or three impacts with a 24 hour inter-injury periodicity caused a reduced latency to find the hidden platform on the Morris water maze, which suggests a learning or acquisition deficit. We also observed increased anxiety as compared to uninjured mice in animals that received 3 mTBIs. In summary, FE modeling of axon geometry and related blast profiles for models are					
15. SUBJECT TERMS Mild traumatic brain injury, finite element analysis, axonal geometry, repetitive injury					
16. SECURITY CLASSIFICATION OF:			17. LIMITATION OF ABSTRACT UU	18. NUMBER OF PAGES 29	19a. NAME OF RESPONSIBLE PERSON USARMRC
a. REPORT U	b. ABSTRACT U	c. THIS PAGE U			19b. TELEPHONE NUMBER (include area code)

Table of Contents

	<u>Page</u>
Introduction.....	4
Body.....	4
Key Research Accomplishments.....	13
Reportable Outcomes.....	14
Conclusion.....	14
References.....	15
Appendix: Abstracts.....	17
Appendix: Supporting Data.....	18

Introduction:

The purpose of this research is to determine through analytical modeling and animal-based experiments the blast-level threshold for mild traumatic brain injury in humans. Mild traumatic brain injury (mTBI) is known to occur in humans subjected to explosive blast levels that do not induce external or measurable internal injuries. As a result, it is not known until a later date the mTBI has been experienced. Through analytical modeling in this research, the blast-induced internal strain and rates of strain in the human brain are going to be determined. Determining these levels will be accomplished by simulating the structure of the brain subjected to blast levels found in the literature. Then, corresponding mouse brain models will be developed in order to determine the analogous response parameters in those scaled brains. In a tandem effort, laboratory-based animal experiments are being conducted to determine the blast-pressures and impact-acceleration parameters that induce mTBI in mice. Once the impact-acceleration and blast levels that cause mTBI in animals are understood, it will be possible to use the animal-based analytical models to determine the corresponding brain response parameters. These brain response parameters will then be scaled to the human brain analytical modeling so that the blast pressures that generate these response rates can be determined.

Body:

This section provides an overview of the work and accomplishments. The approved tasks from the Statement of Work are provided in *italics*. Below those statements, the corresponding progress from June 2009-June 2010 is detailed. Statements are also made with regard to work in progress or that has yet to be done.

Statement of Work:

To test the hypotheses, and numerical simulations and animal-based experiments will be conducted. The specific aims, as described in this proposal, will be achieved by collaborative research between the Department of Physical Medicine and Rehabilitation at The University of Alabama at Birmingham (UAB) and the Department of Mechanical Engineering at The University of Alabama (UA). UAB and UA are only about 50 miles apart, which will facilitate convenient and frequent meetings between the two groups. The specific tasks to reach the research aims include:

Task 1: Initialization of project and organization of collaborative team

This task has been completed. Frequent email and phone correspondence occurs between the collaborative teams with quarterly group meetings held to transfer ideas and discuss progress.

Task 2: Simulation of full-scale blast scenarios using a dynamic model

Brain injuries have a direct impact on the quality of life for those affected as well as an indirect, and significant, impact resulting from the health care of injured individuals. As a result, obtaining a basic understanding of the mechanisms that produce brain injury has been the goal of research for many decades. Some of the earlier studies focused on assessing concussions and scaling animal-based experiments to humans¹⁻³. Because of the obvious issues associated with testing humans, there has been a consistent interest in obtaining the mechanical properties of

both animal and human brain tissues⁴⁻¹³. By having these tissue properties, engineers and scientists have utilized analytical and numerical modeling approaches to gain a better understanding of the mechanisms that generate brain injury^{3,14-23}. Some of these brain injury studies have gone so far as to find mechanical thresholds that are believed to characterize the onset of brain injury^{18,20,23-29}. Recent work has focused on correlating mechanical inputs known to cause injury with internal responses of the brain found using finite element modeling. Strain and strain rates within the brain have been shown to be an indicator of a probability of injury²⁶. By using injuries observed from football players, that work was extended to establish a tolerance level that predicts concussions²⁷. The latter work utilized the Wayne State Brain Injury Model (WSUBIM) to determine the shear strain levels in the midbrain region believed to induce mild traumatic brain injury (mTBI). Other work has also involved correlating experimental data with results found using detailed finite element models of the human head^{20,23,29}.

While the models described above attempt to obtain a mechanical threshold criteria associated with the onset of brain injury, there are some important limitations that must be understood before using the results to better understand the onset of injury. It is clear that a great deal of effort has gone into developing complex models of the human head. In the brain portion of these models, though, both the white matter and gray matter were represented as homogeneous materials. Although some indication of the level of strain, or strain rate, that produces injury may be obtained, the underlying mechanisms that produce that injury can not be understood any better than before. It is well known that cells within the brain contain several different types of components. For example, the axons that transmit information through the brain contain microtubules and neurofilaments³⁰. These rod-like components provide important structural support and transport pathways that help maintain the axons ability to function³¹. Because the modeling methods described above do not include these microscopic components, there is no means of assessing the impact that mechanical forces have on these components. Because the health of axons is known to depend on these components, the goal of the work described here is to continue the examination of brain injury modeling, but from a more microscopic perspective.

Of course, in developing a model of these microscopic components, one must have a detailed understanding of the various components structures and properties³². In the last several decades, various researchers have examined the structure and material properties of microtubules^{6,33-44}. As a result, the microtubule seems a good candidate for this initial study of the fundamental brain failure mechanisms. While the failure of neurofilaments and other components may also play a role in brain injury, the study of those components will be described in detail in later work. Certainly, knowing the geometry and material properties of microtubules, as well as the surrounding cytoplasm, are important in modeling these microstructures. Nevertheless, these new models will not provide additional insight unless some criteria are available for determining structural failure within that component. Recent work by de Pablo *et. al.*⁴⁰ and Schaap *et. al.*^{41,43} concentrated on using atomic force microscopy to measure the elastic properties of microtubules. They were able to provide a fairly concise assessment of the elastic properties of microtubules. An even more significant observation in their work was that when a radial scanning load greater than 300 pN was applied to the microtubule, the structure would collapse irreversibly, beyond the point of self-repair. This force, although approximate, provides the important starting point to begin the numerical study of failure mechanisms within a brain microstructure.

Perhaps the most important work related to the present study is the more recent work of Schaap et. al.⁴³. That study examined in more detail the radial load that generates structural failure as well as the modeling requirements for a microtubule. Beyond the simple thin-shell model and three dimensional solid-wall cylindrical model used to represent microtubules, that work also examined a cylindrical structure with ribs. The latter was used to assess the impact of including the shapes of the protofilament chains that make up the walls of the microtubule. Having the basic understanding of the accuracy of these models, provides a good basis for the research being addressed in the current work.

As noted above, the goal of the current work is to examine the failure of brain components from a microscopic level. To that end, this new approach will initially focus on assessing the structural failure of microtubules (MTs) within the brain. In the first part of the study, a more generic understanding of the onset of MT failure will be obtained. This will be accomplished by modeling the MT in order to determine the internal stresses the results when the 300 pN failure load are applied. Once a maximum stress level associated with the 300 pN radial load is obtained, that stress will serve as the strength of the microtubule throughout the remainder of the study. Then, a three dimensional model of a microtubule suspended in cytoplasm will be developed. That model will enable the stresses within the MT to be computed as pressure waves propagate through the medium containing the MT. Because a transient analysis is being used, only the wave that initially passes through the material will be of interest. As a result, the boundary conditions on the surrounding materials will not be important due to the sonic speed of the traveling waves. By using the strength criteria, it will then be possible to determine the pressure levels within the brain that produce MT structural failure.

Prior to describing the work, some limitations of the present work should be noted. First, it is not expected that exact values for the failure of MTs will be obtained. It is understood that the properties of MTs can vary depending on the particular loading of interest (normal vs. shear)⁴⁴. Furthermore, the properties of brain materials can vary in a viscoelastic manner frequency^{5,13,45,46}. By using a stress-based approach, though, the absolute values of the material properties (i.e. Young's modulus) will not be so critical. So long as the relative material properties are approximately valid, then the relative stresses that will results should be reasonable. Again, the goal of this initial work is to begin the process of studying these important failure mechanisms and how they may contribute to mTBI. Future work will focus other microscopic structures, as well as structures that may attach to MTs and the associated loadings that can occur from the presence of these components. It is hoped that this new approach to studying brain injury will provide motivation to better measure the failure mechanisms of these microscopic components in the laboratory. While these structures are not necessarily homogenous in nature, it is hoped that an appropriate homogenous model can provide useful insight into the failure mechanisms. Furthermore, studies that determine the physiological consequences of these microscopic failures can be conducted with greater confidence.

Prior to describing the work, some limitations of the present work should be noted. First, it is not expected that exact values for the failure of MTs will be obtained. It is understood that the properties of MTs can vary depending on the particular loading of interest (normal vs. shear)⁴⁴.

Furthermore, the properties of brain materials can vary in a viscoelastic manner frequency^{5,13,45,46}. By using a stress-based approach, though, the absolute values of the material properties (i.e. Young's modulus) will not be so critical. So long as the relative material properties are approximately valid, then the relative stresses that will results should be reasonable. Again, the goal of this initial work is to begin the process of studying these important failure mechanisms and how they may contribute to m TBI. Future work will focus on other microscopic structures, as well as structures that may attach to MTs and the associated loadings that can occur from the presence of these components. It is hoped that this new approach to studying brain injury will provide motivation to better measure the failure mechanisms of these microscopic components in the laboratory. While these structures are not necessarily homogenous in nature, it is hoped that an appropriate homogenous model can provide useful insight into the failure mechanisms. Furthermore, studies that determine the physiological consequences of these microscopic failures can be conducted with greater confidence.

MICROTUBULE STRENGTH

The work of Schaap *et al.*⁴³ is used as a starting point in determining a strength associated with microtubules (MTs). That work states "Collapse of the tubes is expected when the stress exceeds the ultimate strength of the material. For the MT, this happened at tip forces $< \sim 0.3$ nN." That work also noted various mechanisms that might occur at the onset of failure, such as the dislocation of tubulin bonds. Nevertheless, no additional insight was provided with regard to a strength associated with MTs. As a result, the initial goal of this work is to determine an equivalent MT strength. Once that strength has been determined, it will be possible to then determine the mechanical loading conditions that produce stresses that exceed the MT strength.

A three dimensional cylindrical finite element model with a radial point load is used to estimate a strength for MTs. The 13 protofilaments that make up the walls of a typical MT produce a geometry that is more realistically treated as a ribbed cylinder. A discussion regarding the validity of different types of linearly elastic models is provided in Reference 43. A uniform cylinder with an internal diameter of 16.8 nm and an effective wall thickness of 1.54 nm was shown to provide some of the expected elastic properties. As a result, that uniform cylinder will be examined here, with the intent of evaluating more realistic geometries in future work. As a result, a 3-d solid elements FE model with young's modulus of 2.2 GPa is examined with a 300 pN static radial load, as illustrated in Figure 1(a). From Fig.1 (b), it can be seen that the maximum stress value is 0.172GPa, which is at the tip force loading location on the microtubule cylinder structure. Based on this analysis, this stress will be assumed to be that associated with permanent deformation and microtubule injury.

TRANSIENT WAVE LOADING IN MICROTUBULES LEADING TO FAILURE

The infinite MT filled with cytoplasm and finite length MT with cytoplasm have been analyzed by using ANSYS FEM tools to reveal maximum stress values which will yield the MT cylinder structure when subjected to a pressure load impacted with a time period of 1.03095×10^{-8} s. A stress wave propagation caused by this pressure load will travel through MT and cytoplasm assembly. The material properties in Young's modulus of microtubule are 2.2 GPa, MT density at 1040 kgm^{-3} and Poisson ratio 0.3. For the surrounding cytoplasm medium, Young's modulus is

1kPa, density is 1040 kgm^{-3} and Poisson ratio is 0.499. As expected, the maximum stress values in the microtubules occurs when the wave loads pass through. In these FEM models, all elements are solids. These models were applied by a pressure load of 0.13GPa at the side surface close to the microtubule structure and produce stress waves propagating along the x direction of the model. Figures 2a and 2b clearly show that maximum stress values appear at the microtubule structure at two different times, they are 1.32 GPa at time 2.89×10^{-09} s and 3.32 GPa at time 1.03×10^{-07} s. These values have exceeded the yield stress value 0.172GPa, which cause the permanent deformation inside microtubule structure under this pressure impact. Figures 3(a)~(c) show that stress waves travel along x direction from one side to another, due to the reason that microtubule structure immersed inside cytoplasm media with $48\text{nm} \times 40\text{nm} \times 100\text{nm}$. The stress distribution at each time is shown for cytoplasm media, which is much lower than that of microtubule structure. Figure 4 shows stress wave propagation inside the cytoplasm medium, which is much lower than that of microtubule structure, by comparing with Figure 5 which shows stress wave propagation at whole infinite length microtubule with cytoplasm media. Also, the finite length microtubule with cytoplasm media beam as illustrated in Fig.2 has much larger stress values than infinite length microtubule assembly shown in Fig.5 under the same applied pressure loads.

Task 3: Characterize fundamental parameters for dynamic mouse model of mTBI using an impact acceleration model

Our work from the preceding year indicated that a single impact-acceleration injury of 0.058, 0.096 or 0.196 Joules (J) in adult, male mice did not produce behavioral and histological outcomes that reliably indicated the occurrence of mild traumatic brain injury. Thus, these impact acceleration injury magnitudes were determined to be minor. Therefore, we evaluated the effects of a 0.588J impact-acceleration model which is induced by dropping a 100g weight from a height of 60cm to impact a steel disk affixed to the skull of an adult mouse, as detailed below. The effects on duration of loss of consciousness (as measured by duration of transient unconsciousness), post-impact vestibular motor performance (as measured by Rotorod performance), post-impact learning and memory (as measured by performance in the Morris Water Maze), and post-impact anxiety (as measured by performance in the elevated plus maze) were measured.

A. Induction of Impact-acceleration brain injury: Adult, male C57BL6 mice were anesthetized in an induction chamber with 4% isoflurane for 4 minutes, followed by a maintenance dose of 2.5% isoflurane administered via nose cone for the remainder of the surgical procedure. The scalp of each mouse was shaved and scrubbed with betadine and chlorhexidine prior to receiving a midline scalp incision. The skin and fascia were reflected such that the central, bregma, and lambda skull sutures were clearly visible and hemostasis was achieved prior to impact. A stainless steel disk (3mm diameter, 0.5mm thickness) was affixed with cyanoacrylate glue to the mouse skull. The mouse was removed from the nose cone and positioned on the foam support block underneath the weight-drop device. A 100g stainless steel weight (4.5mm outer diameter) with a conical tip (3.5mm outer diameter) was dropped from 60 cm through a Plexiglas tube (5.0mm inner diameter) onto the steel disk affixed to the mouse skull. The impact site was centered on the central suture equidistant between the bregma and lambda skull sutures. The

mouse was quickly removed from the foam pad to avoid any rebound injury from the weight after the impact. The induction of skull fracture and hematoma were carefully examined after each impact. Each mouse received only one impact.

B. Evaluation of behavioral outcomes:

1. Effect of 0.588 J impact-acceleration brain injury on duration of loss of consciousness:

When a conscious rodent is placed on its back, it will roll or flip to its feet to “right” itself and the time to return of the righting reflex after mTBI was recorded as an indicator of loss of consciousness (transient unconsciousness). Previous research indicates that duration of transient unconsciousness correlates with injury severity in both the clinic⁴⁷ and the laboratory⁴⁸. As shown in figure 6, we found that 0.588 J impact-acceleration injury induced a significantly longer duration of transient unconsciousness $\{t(1,9) = 4.175, p < 0.001\}$ as compared to mice in the sham group (uninjured mice). These data suggest that skull was impacted with sufficient force to induce a brain injury.

2. Effect of 0.588 J impact-acceleration brain injury on acute post-impact vestibular motor performance:

Each mouse was placed individually on a 5cm wheel with rungs on the surface for grip. The wheel rotates in a single direction and gradually increases in speed until reaching a maximum speed of 20rpm in 90sec. The mouse must maintain balance and walk on the wheel to avoid falling onto a pad below. The latency to remain on the rotating rod before falling is an indicator of balance and vestibular motor function. Rotorod performance is very sensitive to vestibular motor deficits after TBI⁴⁹. Baseline rotorod performance was evaluated one day prior to the induction of the impact-acceleration injury and on days 1, 2, and 3 post-impact. As shown in figure 7, no statistical differences were detected between mice in the sham (uninjured) and impact-acceleration TBI groups with an $n = 9$ animals per group. An additional 6 mice per group will be added to achieve the necessary statistical power, but it is anticipated that the results will change much upon additional of the additional animals. Thus, these data suggest that a single 0.588 J impact-acceleration brain injury does not induce vestibular motor deficits as detected by the rotorod task.

3. Effect of 0.588 J impact-acceleration brain injury on learning and memory:

Learning and memory after impact-acceleration brain injury were evaluated using the Morris water maze on post-impact days 6-10. In the water maze, animals must swim to find a non-visible 10cm platform submerged 0.5cm under the surface of the water in a 1.2m diameter pool. As the mouse swims, its path and latency to find the platform were recorded by software assisted video tracking system (Ethovision, Noldus, Inc.). Each mouse was given 4 trials per day for 5 days with each trial beginning at a random start position (i.e. north, east, south, west). The mouse uses contextual cues in the room to learn and remember the location of the hidden platform. The latency to find the platform and the time spent in the quadrant of the platform upon probe trial are indicators of learning and memory, respectively. As seen in figure 8, the latency to find the hidden platform was not statistically different between uninjured sham mice and mice that received the impact-acceleration injury. Although we noted that the mice in the sham group of this experiment took nearly 20 seconds longer to find the platform than mice in the sham group of our other experiments, the MW M latency data collected to date in this experiment suggest that impact-acceleration brain injury did not induce a statistically significant

difference in learning. We also evaluated the performance of each mouse in a probe trial. In the probe trial all the conditions remained the same except that the hidden platform is removed from the water maze. The probe trial was performed after the completion of the final set of trials on trial day 5 (post-impact day 10). The amount of time a mouse spends in the quadrant where the platform was formerly located is an indicator of memory. As shown in figure 9, we found that all mice, regardless of injury condition, spent nearly half of the time in the pool searching the quadrant where the platform was previously located. This suggests that mice in all groups learned the location of the hidden platform by using spatial cues and retained this memory on trial day 5. An important control in evaluating MWM performance is to measure the swim speed of all animals (table 2). We found that swim speed did not differ between injury groups or evaluation days, which suggests that motor and or swimming ability was the same between experimental groups.

4. Effect of 0.588 J impact-acceleration brain injury on anxiety: State anxiety was assessed by measuring time spent in open vs. closed arms in the elevated plus-maze on post-injury day 6 (figures 10-12). The maze is constructed of 4 plastic arms (20cm) at right angles to each other connected by a central square. Two of the opposite arms are referred to as closed arms and are enclosed by a high wall (15cm) and the two open arms have a 0.5cm ridge. The maze is elevated (50cm) above the floor. The mouse is placed in the center, facing a closed arm. As the mouse moves, the time spent in the open and closed arms, rearing, and total movement time are recorded by a software assisted tracking system (Ethovision, Noldus, Inc.). This test is a reliable and validated measure of anxiety. Anxiolytic effects are indicated by increased time and/or rearing in the open arms and anxiogenic effects are indicated by decreased time and/or rearing in open arms. Mice that received an impact-acceleration brain injury spent significantly less time in the open arms than uninjured (sham) mice (figure 10). Similarly, mice that received an impact-acceleration brain injury exhibited reduced rearing in the open arms (figure 11). An important control is to evaluate the motor ability of each group to determine that both groups could perform the task equally. This was done by evaluation of the total time spent moving (figure 12). No differences between experimental groups, which indicates that time spent in the arms was not influenced by difference in motor ability. Taken together, these data suggest that impact-acceleration brain injury increased state anxiety in adult male mice.

Task 4: Study loading on the brain via simulation

This is work to be done in 2010-2011 and the foundations for this work are currently being completed in task 2.

Task 5: Develop a dynamic mouse model of blast injury

As this initial work for this task also relates to task 7, the data from the prototype mouse model will be presented under task 7. The foundations for this are currently being investigated and this task will be a focus of the next year's research.

Task 6: Development of test system and fixture configurations

Similar to Task 5, this will be a focus of next year's research, but preliminary design and development of a test system and fixture configuration has been initiated. Feasibility was evaluated in preliminary field testing (figure 13) of detonation of a commercially-available,

standardized charge (.22 caliber Hilti explosive cartridge rated at 385, 490, 575 ft/sec velocity) via a modified Hilti DX E72 into a PVC cylinder (2 in. inside diameter; 1, 2, or 3 ft. length). The Hilti DXE72 was modified by removing the internal piston. It was determined that detonation of the standardized charges was reproducible and that detonation into the PVC cylinder did not exceed material tolerance limits. Subsequently, evaluation of the 2 ft. prototype detonation configuration was conducted in a hemi-anechoic chamber (<http://www.me.ua.edu/stal/>) and the maximum pressure at exhaust was measured by microphone and pressure sensors. It was determined the peak pressure at exhaust was 60 kPa with the 385 velocity charge and 80 kPa with the 575 velocity charge. Further development and testing of fixture and configurations is underway. Figure 14 shows a design idea currently being discussed and prototyped. This work will continue into the next year and will be an area of great emphasis.

Task 7: Determine if single or multiple blast exposures in a mouse confer signs and symptoms similar to those of human mild TBI

This work is on-going and procedures will be updated and modified in collaboration with the data obtained in tasks 4-6, but preliminary evaluation has begun as detailed below.

A. Exposure to blast-overpressure: Adult, male C57BL6 mice were anesthetized in an induction chamber with 4% isoflurane for 4 minutes. Mice were then removed to room air and placed into a custom-build restraint apparatus which immobilized the head and constrained the body by use of padding and protective straps. The eyes were protected by black, light absorbing cloth strips. Each mouse was positioned at the end of a 5ft. long PVC chamber (5 in. inside diameter) such that only the head is exposed to the chamber and that the top of the head is perpendicular to the detonation source. The procedure to place the mouse into the restraint apparatus takes >30 sec. A modified Hilti DX E72 was used to detonate a .022 caliber 490 ft./sec. cartridge at a distance of 5 ft. from the mouse head into the PVC chamber. After detonation, each mouse was rapidly removed from the restraints and evaluated for duration of transient unconsciousness.

B. Behavioral outcome measures:

1. Effect of blast-exposure on duration of loss of consciousness: Righting time was measured as described above. Interestingly and as shown in figure 15, righting time did not differ significantly between sham and blast-exposed mice which suggests that blast-exposure at this magnitude did not induce loss of consciousness. However, we observed acute post-blast alterations in consciousness that we have not previously observed in the impact-acceleration injury model or in the fluid percussion model in mice or rats (unpublished observation). We observed that after blast-exposed mice regained the righting response, the animal would sit immobilized and non-responsive for several seconds (>15 sec.), followed by a brief (< 5 sec.) activity and then another period of immobility (>15 sec.). This cycle would repeat several times for each mouse. In order to evaluate the duration of this altered state of consciousness, three additional behavioral parameters were operationally defined and evaluated as follows:

a) auditory response: the time until mice responded to an auditory stimulus in which a response was defined as a flinch or rapid head movement immediately after a snap generated by a ungloved, human hand administered 3 cm above the pinna of the ear. The

stimulus was administered in 15 second intervals beginning immediately after the righting response occurred.

b) tactile response: the time until the mouse responded by a flinch or rapid head movement to a brushing of the whiskers with the tip of a cotton swab was recorded. The stimulus was administered in 15 second intervals beginning 15 seconds after the righting response occurred.

c) dazed: the time until the animals initiates and maintains ambulation and spontaneous exploratory behavior in an open field for 15 continuous seconds.

Also as seen in figure 15, the return of auditory response, tactile response, and duration of dazed behavior was simultaneous with the return of righting response in the sham mice. However, blast-exposure induced a significant increase in time until return of the auditory response, tactical response and termination of the dazed behavioral profile.

2. Effect of head only blast-exposure on acute post-blast vestibular motor performance:

Each mouse was evaluated on the Rotorod task as described above on post-blast exposure days 1-3. Baseline Rotorod performance was evaluated one day prior to the blast-exposure. As shown in figure 16, blast-exposure caused a reduction in the latency to remain on the rod as compared to uninjured mice (sham) on post-exposure days 1 and 3 post-exposure, with a trend toward a decrease in latency on day 2. An additional 6 mice per group will be added to achieve the necessary statistical power, however these data preliminarily indicate that blast exposure induces alteration in vestibular motor performance.

3. Effect of head only blast-exposure on learning and memory:

Learning and memory after head only blast exposure was evaluated using the Morris water maze on post-exposure 6-10, as described above. The latency to find the platform and the time spent in the quadrant of the platform upon probe trial are indicators of learning and memory, respectively. As seen in figure 17, the latency to find the hidden platform was not statistically different between uninjured sham mice and mice that received the impact-acceleration injury. We also evaluated the performance of each mouse in a probe trial as described above. As shown in figure 18, we found no significant differences between the control (sham) group and the blast-exposed group which suggests that mice in all groups learned the location of the hidden platform by using spatial cues and retained this memory on trial day 5. An important control in evaluating MWM performance is to measure the swim speed of all animals (table 3). We found that swim speed did not differ between injury groups or evaluation days, which suggest that motor and or swimming ability was the same between experimental groups.

4. Effect of head only blast-exposure on anxiety: State anxiety was assessed by measuring time spent in open vs. closed arms in the elevated plus-maze on post-exposure day 6 as described above. Anxiolytic effects are indicated by increased time and/or rearing in the open arms and anxiogenic effects are indicated by decreased time and/or rearing in open arms. Mice that received a head only blast-exposure spent significantly less time in the open arms than uninjured (sham) mice (figure 19). Similarly, mice that received an head only blast exposure exhibited reduced rearing in the open arms (figure 20). An important control is to evaluate the motor ability of each group to determine that both groups could perform the task equally. This was done by evaluation of the total time spent moving (figure 21). No differences between

experimental groups, which indicates that time spent in the arms was not influenced by difference in motor ability. Taken together, these data suggest that head only blast-exposure increased state anxiety in adult male mice.

Task 8: Evaluation/ optimization of fixture construction, load generation of mouse blast apparatus

This work has not been initiated, but is planned for 2010-2011.

Task 9: Evaluate the cortex, hippocampus, thalamus, cerebellum, and amygdala of mice exposed to single or multiple sub-lethal blast exposure for pathological indicators of brain trauma

This work has been initiated, but is still ongoing. Several tissue specimens have been processed for histochemistry and example micrographs from brain sections processed with cresyl violet histochemistry (figure 22), Fluoro jade B (figure 23), and assayed for immunoreactivity to GFAP (figure 24) are included. No quantification has yet been conducted, but those experiments are planned. Also, histological markers of diffuse axonal injury will be critically evaluated, as the modeling data suggests that may be the first pathological consequence of blast exposure.

Key Research Accomplishments:

- Estimation of the static compression results that produce some permanent deformation of MT
- Modeling of pressure wave propagation through the MT and calculation of stress as related to yield strength
- Prediction of blast-induced permanent damage to the MT
- Estimate of resulting stresses in the cytoplasm, based on the assumed geometry, and comparison to stresses in MT
- Estimation of Von Mises under various load conditions
- Evaluation of 0.588 J impact-acceleration injury in adult male mice with regard to duration of transient unconsciousness, vestibular motor performance, alterations in learning and memory, and effects on anxiety
- Design, and prototyping of mouse blast fixture using a commercially available detonation source
- Evaluation of head only blast exposure in adult male mice with regard to duration of transient unconsciousness and alterations in consciousness, vestibular motor performance, alterations in learning and memory, and effects on anxiety
- Evaluation of histological markers of injury after head only blast exposure

Reportable Outcomes:

- Abstract: Biao B. (Bill) Zhang and William S. Shepard Jr., Candace L. Floyd. Investigation of stress wave propagation in brain tissues through the use of finite element method. ASME 2010
- Abstract: Candace Floyd. Translating TBI/SCI *in vitro* models to animal models. National Neurotrauma Society 2010

Conclusion:

Axon injuries have been noted in previous research works. Due to the complicated structure as well as a lack of understanding regarding the types of loading that potentially result in structural failure, a complete understanding of axonal failure is still lacking. In this portion of the research, stress waves propagating through a microtubule structure resting in a cytoplasm matrix have been examined. The model was constructed based on the findings of other researchers. Furthermore, experimental loads found by others that result in collapse of the MT structure were used as a basis in this portion of the work for estimating a yield strength associated with the MT structure. Refinements of that analysis are needed in the next portion of the work. Nevertheless, the basic formulation has been completed so that further work can continue.

One of the most important outcomes of this approach is the likely ability to translate simulation results directly to experimental verifications. Because the models developed are for fundamental structures within the brain, the need for scaling between animal-based experiments and estimates for human levels may not be necessary. This is a fundamentally different approach than what has been used previously. For a wave propagating perpendicular to the MT axis, pressure loads have been found that cause the stresses in the MT structure to exceed the estimated yield stress. Two conditions were considered in the simulations reported here. In one condition, the MT was completely encapsulated within the cytoplasm. This case mimics a finite length MT. In another study, the cytoplasm structure ended at the end of the MT. This latter case is used to simulate the effects in longer MT structures. Of course, to fully understand the mechanics and important loading conditions, other wave propagation directions will need to be considered, such as axial and oblique loading. Further refinements to the model, such as the possibility of incorporating ribs to mimic the filaments that make up the MT, are also needed to better improve the simulation results. These areas will be the subject of upcoming work in the area.

With regard to the mouse model and animal experimentation, we have found that 0.588 J impact-acceleration injury produces a brain injury with mild symptomatology. Specifically we report that this level of impact-acceleration injury induces transient loss of consciousness but does not induce lasting vestibular motor deficits acutely after injury. In comparison, a head only blast exposure did not induce transient loss of consciousness, but instead induced transient alterations in consciousness. Also, the head only blast exposure preliminary evaluated here induced acute alterations in vestibular motor function. Neither the impact-acceleration injury nor the head only blast-exposure induced significant deficits in learning and memory as detectable by the evaluation in the Morris Water Maze. It is possible that this task is not sensitive enough in mice to discern the level of learning and memory deficits induced by mild brain injury, however more mice need to be evaluated before this interpretation is solidified. It was also noted that several of the mice in our sham group had very poor performance in this task, and that needs to be further evaluated. Additionally we report here that both the impact-acceleration injury and blast-exposure induced state anxiety in the mice as measured in the elevated plus maze. Lastly, we have begun to examine several histological markers of injury in brains from mice exposed to impact-acceleration or blast-exposure and this work will continue in earnest.

References:

1. A. G. Gross, "Impact thresholds of brain concussion," *J. Aviation Med.*, **29**(10), pp. 725-732 (1958).
2. A. K. Om maya, P. Yarnell, A. E. Hirsch and E. H. Harris, "Scaling of experimental data on cerebral concussion in sub-human primates to concussion threshold for man," in *Proceedings of 11th Stapp Car Crash Conference* (New York, 1967) 670906, pp. 47-52.
3. Y. K. Liu and K. B. Chandran, "The exact solution for the translational acceleration of fluid-filled rigid spherical shells - A model for the development of intracranial pressure," *Mathematical Biosciences*, **24**, pp. 1-16 (1975).
4. G. T. Fallenstein, V. D. Hulce and J. W. Melvin, "Dynamic mechanical properties of human brain tissue," *J. Biomechanics*, **2**(3), pp. 217-226 (1969).
5. J. E. Galford and J. H. McElhane, "Some viscoelastic properties of scalp, brain, and dura," in *Proceedings of ASME Meeting 69-BHF-7* (Ann Arbor, MI, 1969), pp. 8.
6. M. Sato, W. A. Schwartz, S. C. Selden and T. D. Pollard, "Mechanical properties of brain tubulin and microtubules," *J. Cell. Bio.*, **106**(4), pp. 1205-1211 (1988).
7. J. A. Galbraith, L. E. Thibault and D. R. Matteson, "Mechanical and electrical responses of the squid giant axon to simple elongation," *J. Biomech. Eng.*, **115**(1), pp. 13-22 (1993).
8. B. R. Donnelly and J. Medige, "Shear properties of human brain tissue," *J. Biomech. Eng.*, **119**(4), pp. 423-432 (1997).
9. K. Miller, K. Chinzei, G. Orsengo and P. Bednarz, "Mechanical properties of brain tissue in-vivo: experiment and computer simulation," *J. Biomechanics*, **33**(11), pp. 1369-1376 (2000).
10. B. Fabry, G. N. Maksym, J. P. Butler, M. Glogauer, D. Navajas and J. J. Fredberg, "Scaling the microrheology of living cells," *Physical Rev. Letters*, **87**(14), pp. 148102-1-4 (2001).
11. K. Miller and K. Chinzei, "Mechanical properties of brain tissue in tension," *J. Biomechanics*, **35**(4), pp. 483-490 (2002).
12. M. Shafieian and K. Darvish, "Effect of TB I on material properties of rat brain tissue," in *Proceedings of 33rd Annual Northeast Bioengineering Conference, NEBC* (Stony Brook, NY, 2007), pp. 283-284.
13. M. A. Green, L. E. Bilston and R. Sinkus, "In vivo brain viscoelastic properties measured by magnetic resonance elastography," *NMR Biomed.*, **21**(7), pp. 755-764 (2008).
14. J. S. Ruan, T. Khalil and A. I. King, "Dynamic response of the human head to impact by three-dimensional finite element analysis," *J. Biomech. Eng.*, **116**(1), pp. 44-50 (1994).
15. R. Willinger, H.-S. Kang and B. Diaw, "Three-dimensional human head finite-element model validation against two experimental impacts," *Annals Biomedical Eng.*, **27**(3), pp. 403-410 (1999).
16. Y. H. Chu and M. Bottlang, Finite element analysis of traumatic brain injury, Tenth Annual Symposium on Computational Methods in Orthopaedic Biomechanics, (2002).
17. C. S. Cotter, P. K. Smolarkiewicz and I. N. Szczyrba, "A viscoelastic model for brain injuries," *Int. J. Num. Meth. Fluids*, **40**(1-2), pp. 303-311 (2002).
18. S. Kleiven and W. N. Hardy, "Correlation of an FE model of the human head with local brain motion - Consequences for injury prediction," *Stapp Car Crash Journal*, **46**, pp. 123-144 (2002).
19. C. M. Suh, S. H. Kim and W. Goldsmith, "Finite element analysis of brain injury due to head impact," *Int. J. Mod. Phys. B*, **79**(8-9), pp. 1355-1361 (2003).
20. S. Kleiven, "Evaluation of head injury criteria using a finite element model validated against experiments on localized brain motion, intracerebral acceleration, and intracranial pressure," *I. J. Crash.*, **11**(1), pp. 65-79 (2006).
21. H. Mao, L. Zhang, K. H. Yang and A. I. King, "Application of a finite element model to the brain to study traumatic brain injury mechanisms in the rat," *Stapp Car Crash Journal*, **50**, pp. 583-600 (2006).
22. J. Ho and S. Kleiven, "Dynamic response of the brain with vasculature: A three-dimensional computational study," *J. Biomechanics*, **40**(13), pp. 3006-3012 (2007).
23. H. Zou and J. P. Schmiedeler, "Predicting brain injury under impact with a strain measure from analytical models," *I. J. Crash.*, **13**(3), pp. 337-348 (2008).
24. T. A. Gennarelli, "Mechanisms of brain injury," *J. Emerg. Med.*, **11**(Suppl. 1), pp. 5-11 (1993).
25. B. Morrison, III, H. L. Cater, C. C. B. Wang, F. C. Thomas, C. T. Hung, G. A. Ateshian and L. E. Sundstrom, "A tissue level tolerance criterion for living brain developed with an in vitro model of traumatic mechanical loading," *Stapp Car Crash Journal*, **47**, pp. 93-105 (2003).
26. L. Zhang, K. H. Yang, A. I. King and D. C. Viano, A new biomechanical predictor for mild traumatic brain injury - a preliminary finding, Summer Bioengineering Conference, (2003).

27. L. Zhang, K. H. Yang and A. I. King, "A proposed injury threshold for mild traumatic brain injury," *J. Biomech. Eng.*, **126**(2), pp. 226-236 (2004).
 28. K. H. Taber, D. L. Warden and R. A. Hurley, "Blast-related traumatic brain injury: What is known?," *J. Neuropsychiatry Clin Neurosci*, **18**(2), pp. 141-145 (2006).
 29. S. Kleiven, "Biomechanics and thresholds for mTBI in humans," in *Proceedings of IBIA Congress* (Lisbon, Portugal, 2008),
 30. S. G. Waxman, J. D. Kocsis and P. K. Stys, *The Axon: Structure, Function, and Pathophysiology*, p. 692 (1995).
 31. A. Brown, "Slow axonal transport: stop and go traffic in the axon," *Nat. Rev. Mol. Cell Biol.*, **1**(2), pp. 153-156 (2000).
 32. D. A. Fletcher and R. D. Mullins, "Cell mechanics and the cytoskeleton," *Nature*, **463**(7280), pp. 485-492 (2010).
 33. A. Peters and J. E. Vaughn, "Microtubules and filaments in the axons and astrocytes of early postnatal rat optic nerves," *J. Cell. Bio.*, **32**(1), pp. 113-119 (1967).
 34. A. Livingston, "Microtubules in myelinated and unmyelinated axons of rat sciatic nerve," *Cell Tiss. Res.*, **182**(3), pp. 401-407 (1977).
 35. F. Gittes, B. Mickey, J. Nettleton and J. Howard, "Flexural rigidity of microtubules and actin filaments measured from thermal fluctuations in shape," *J. Cell. Bio.*, **120**(4), pp. 923-934 (1993).
 36. M. Elbaum, D. K. Fygenson and A. Libchaber, "Buckling microtubules in vesicles," *Physical Rev. Letters*, **76**(21), pp. 4078-4081 (1996).
 37. H. Felgner, R. Frank and M. Schliwa, "Flexural rigidity of microtubules measured with the use of optical tweezers," *J. Cell Sci.*, **109**(2), pp. 509-516 (1996).
 38. A. Vinckier, C. Dumortier, Y. Engelborghs and L. Hellemans, "Dynamical and mechanical study of immobilized microtubules with atomic force microscopy," *J. Vac. Sci. Technol. B*, **14**(2), pp. 1427-1431 (1996).
 39. A. Kis, S. Kasas, B. Babic, A. J. Kulik, W. Benoit, G. A. D. Briggs, C. Schonenberger, S. Catsicas and L. Forro, "Nanomechanics of microtubules," *Physical Rev. Letters*, **89**(24), pp. 248101-1-4 (2002).
 40. P. J. de Pablo, I. A. T. Schaap, F. C. MacKintosh and C. F. Schmidt, "Deformation and collapse of microtubules on the nanometer scale," *Physical Rev. Letters*, **91**(9), pp. 098101-1-4 (2003).
 41. I. A. T. Schaap, P. J. de Pablo and C. F. Schmidt, "Resolving the molecular structure of microtubules under physiological conditions with scanning force microscopy," *Eur. Biophys. J.*, **33**(5), pp. 462-467 (2004).
 42. C. P. Brangwynne, F. C. MacKintosh, S. Kumar, N. A. Geisse, J. Talbot, L. Mahadevan, K. K. Parker, D. E. Ingber and D. A. Weitz, "Microtubules can bear enhanced compressive loads in living cells because of lateral reinforcement," *J. Cell. Bio.*, **173**(5), pp. 733-741 (2006).
 43. I. A. T. Schaap, C. Carrasco, P. J. de Pablo and F. C. MacKintosh, "Elastic response, buckling, and instability of microtubules under radial indentation," *Biophysical J.*, **91**(4), pp. 1521-1531 (2006).
 44. D. Sept and F. C. MacKintosh, "Microtubule elasticity: Connecting all-atom simulations with continuum mechanics," *Physical Rev. Letters*, **104**(1), pp. 018101-1-4 (2010).
 45. K. K. Darvish and J. R. Crandall, "Nonlinear viscoelastic effects in oscillatory shear deformation of brain tissue," *Med. Eng. & Phys.*, **23**(9), pp. 633-645 (2001).
 46. P. A. Janmey, U. Euteneuer, P. Traub and M. Schliwa, "Viscoelastic properties of vimentin compared with other filamentous biopolymer networks," *J. Cell. Bio.*, **113**(1), pp. 155-160 (1992).
-
- (47) Ruff RM, Iverson GL, Barth JT, Bush SS, Broshek DK. Recommendations for diagnosing a mild traumatic brain injury: a National Academy of Neuropsychology education paper. *Arch Clin Neuropsychol* 2009 February;24(1):3-10.
 - (48) Floyd CL, Golden KM, Black RT, Hamm RJ, Lyeth BG. Craniectomy position affects morris water maze performance and hippocampal cell loss after parasagittal fluid percussion. *J Neurotrauma* 2002 March;19(3):303-16.
 - (49) Hamm RJ. Neurobehavioral assessment of outcome following traumatic brain injury in rats: an evaluation of selected measures. *J Neurotrauma* 2001 November;18(11):1207-16.

Appendices: Abstracts

Investigation of stress wave propagation in brain tissues through the use of finite element method

Biao B. (Bill) Zhang and W. Steve Shepard Jr.

*Dept. of Mechanical Engineering, The University of Alabama, Box 870276,
Tuscaloosa, AL 35487*

Candace L. Floyd

Dept. of Physical Medicine & Rehabilitation, The University of Alabama at Birmingham, Birmingham, AL 35249

Because axons serve as the conduit for signal transmission within the brain, research related to axon damage during brain injury has received much attention in recent years. Although myelinated axons appear as a uniform white matter, the complex structure of axons has not been thoroughly considered in the study of fundamental structural injury mechanisms. Most axons are surrounded by an insulating sheath of myelin. Furthermore, hollow tube-like microtubules provide a form of structural support as well as a means for transport within the axon. There are also discontinuous neurofilaments that serve to strengthen and maintain the axon shape. In this work, the effects of some of these elements on the axon structure are considered in order to obtain a better understanding of wave propagation within the axon. Brain tissues must often be described using complex properties, like viscoelastic or hyperelastic materials, and are often not well characterized. Nevertheless, a means for dealing with some of these issues is considered in an attempt to make progress in this area of brain injury modeling. The goal is to examine axial wave propagation using a simplified finite element analysis so that the impact caused by blast wave loads within the brain axons can be better understood. By conducting a transient analysis, stress and strain distributions as the wave propagates are examined and important characteristics studied. Supported by: DoD CDMRP W81XWH-08-1-0289

Candace Floyd, Ph.D. Abstract/Summary for National Neurotrauma Society 2010 Invited Platform Presentation: Translating TBI/SCI *in vitro* models to animal models

Cell culture models are typically more simplified systems that enable the researcher to investigate the mechanisms, and potential interventions in the pathophysiology of traumatic central nervous system (CNS) injury at a fundamental level. The main *in vitro* model discussed is a mechanical injury model that induces tensile strain, or stretch, in a cell monolayer as originally described by Ellis et al., 1995 (*J. Neurotrauma* Jun;12(3):325-39.). An important aspect in the effective utilization of *in vitro* models in CNS injury research is the translation between cell culture findings and *in vivo* experiments. When used together, *in vitro* and *in vivo* models can be complimentary tools, each with unique advantages. Data on sodium and calcium dynamics in cortical astrocytes after mechanical stretch injury and subsequent manipulation of these pathways *in vivo* after lateral fluid percussion will be discussed. Additionally, our data on stretch injury-induced alterations in expression of inwardly-rectifying potassium currents in spinal cord astrocytes coupled with analysis of these same current after spinal cord injury in adult male rats will highlight several aspects of this approach. Lastly, experimental caveats and limitations in translation between *in vitro* and *in vivo* injury models will be discussed.

Supporting Data:

Table 1 Microtubule material properties [43]

1	MAT Density	1040	kgm^{-3}
2	MAT Poisson's ratio	0.499	-
3	MAT young's modulus	1000	Nm^{-2}
3	MT density	1040	kgm^{-3}
4	MT Poisson's ratio	0.3	-
5	MT young's modulus	2.2	Nm^{-2}

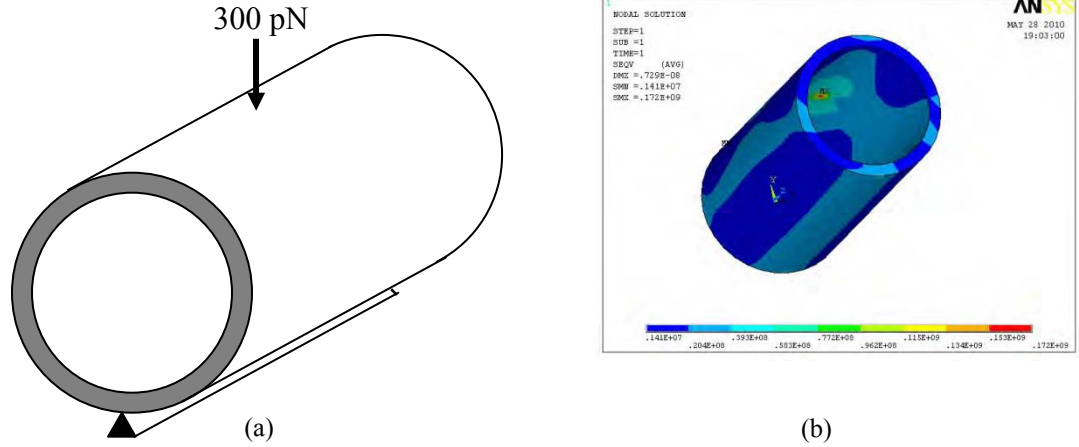


Fig.1 (a) Schematic of uniform cylinder representing MT with 300 pN radial point load, (b) sample simulation stress results (Pa).

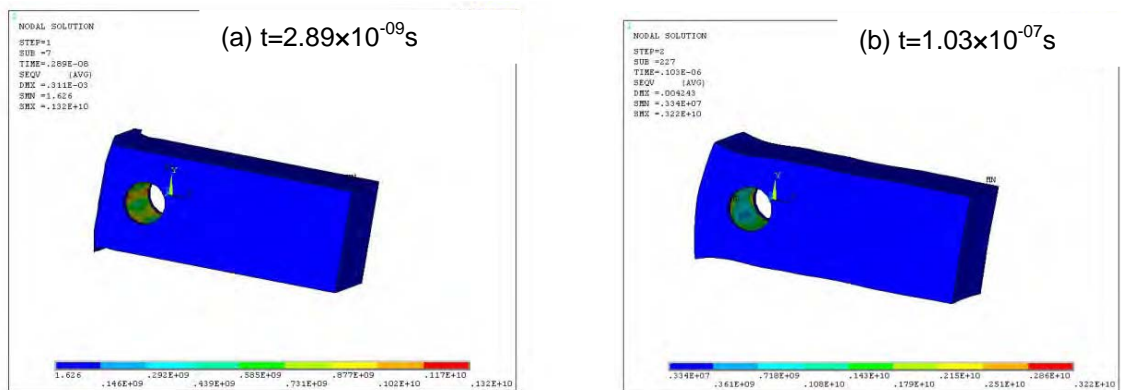


Fig.2 MT with cytoplasm and extending the cytoplasm beyond the MT ends transient stress distribution in Von Mises, the internal and outside cytoplasm elements have been omitted from the figure for clarity

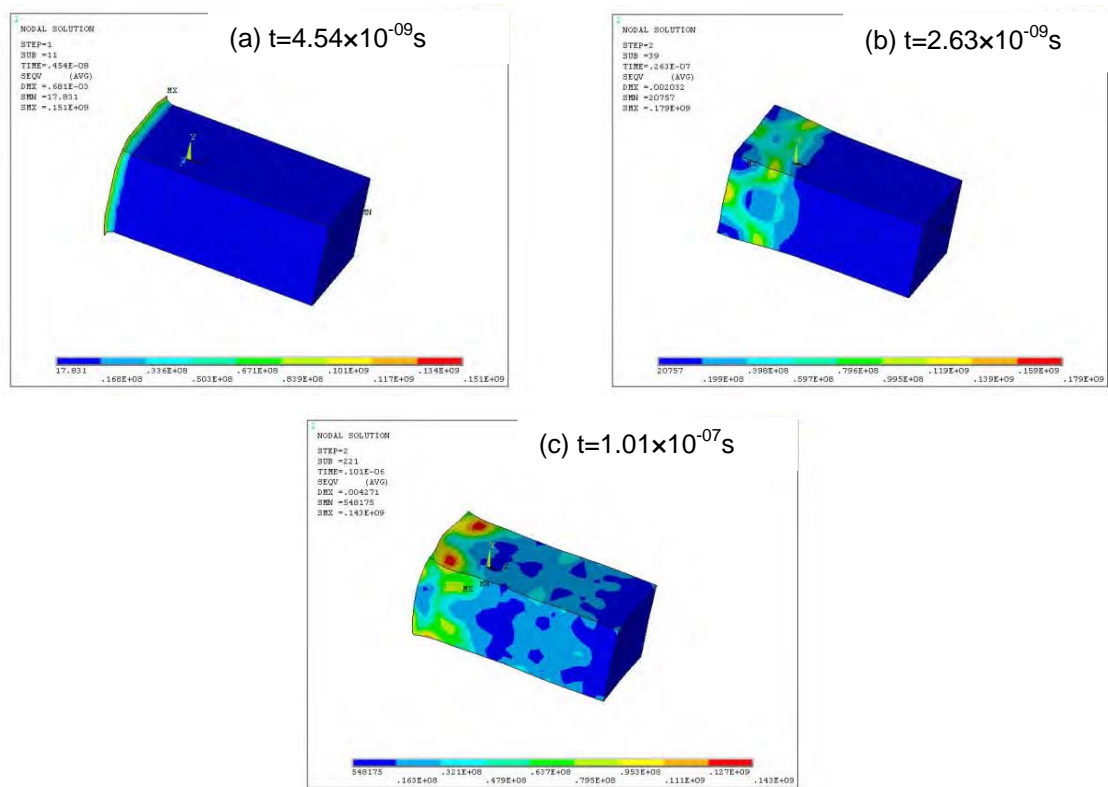


Fig.3 MT with cytoplasm and extending the cytoplasm beyond the MT ends transient stress distribution in Von Mises, the internal microtubule elements have been omitted from the figure for clarity

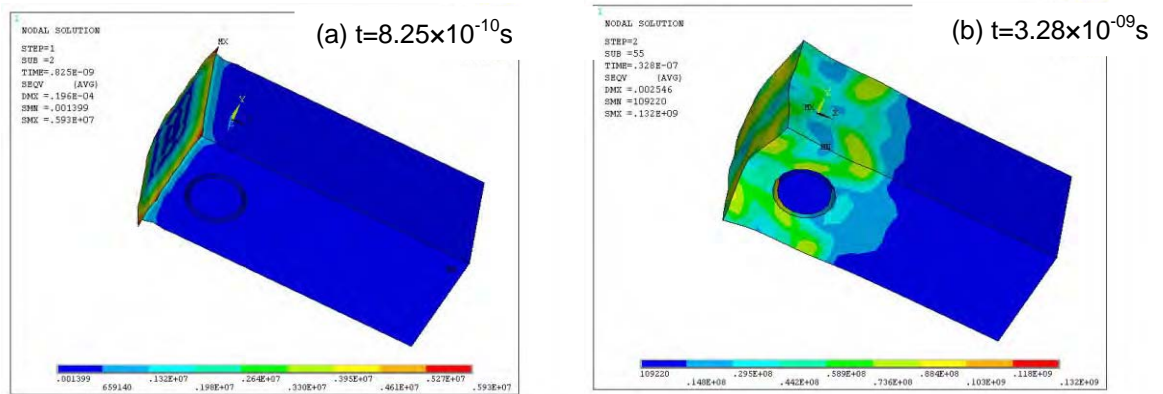


Fig.4 MT with cytoplasm and infinite MT transient stress distribution in Von Mises, the internal microtubule elements have been omitted from the figure for clarity

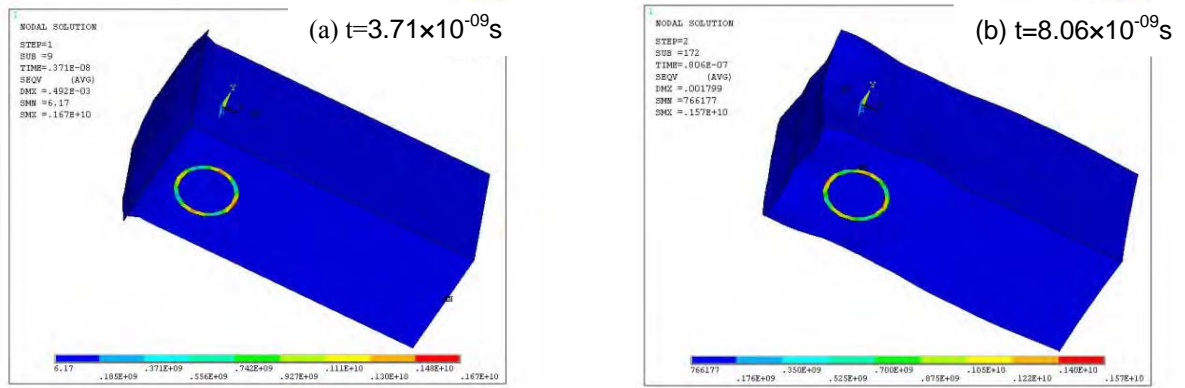


Fig.5 MT filled with cytoplasm and infinite MT transient stress distribution in Von Mises

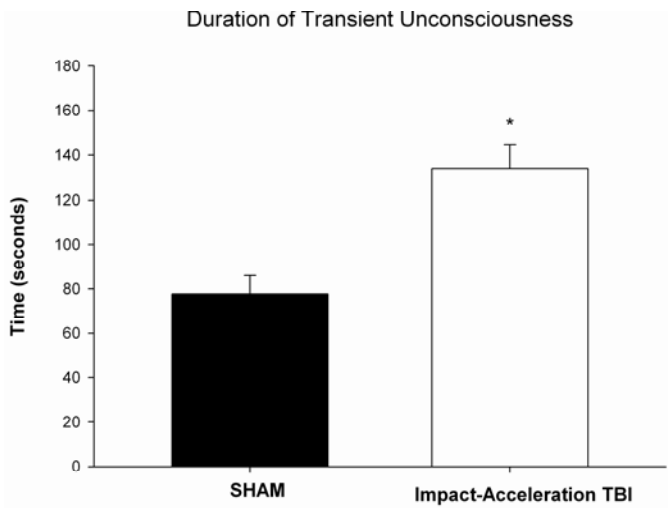


Figure 6: Effect of 0.588J impact on transient unconsciousness. Duration of loss of consciousness (LOC) was measured immediately post-injury. *= injured animals had greater duration LOC than uninjured controls (n=9 per group).

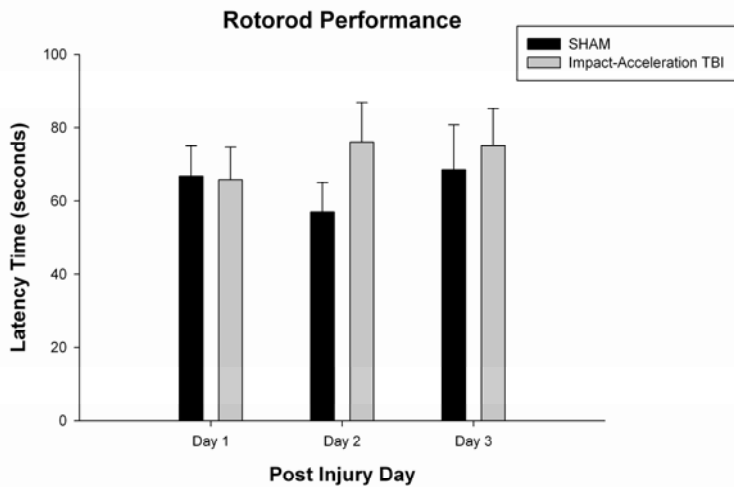


Figure 7: Effect of 0.588J impact-acceleration brain injury on vestibular motor performance. Mice were trained to balance on an accelerating rod, the Rotorod, and latency to fall off was evaluated on post-impact days 1-3. No differences between injury groups were observed (n=9 per group).

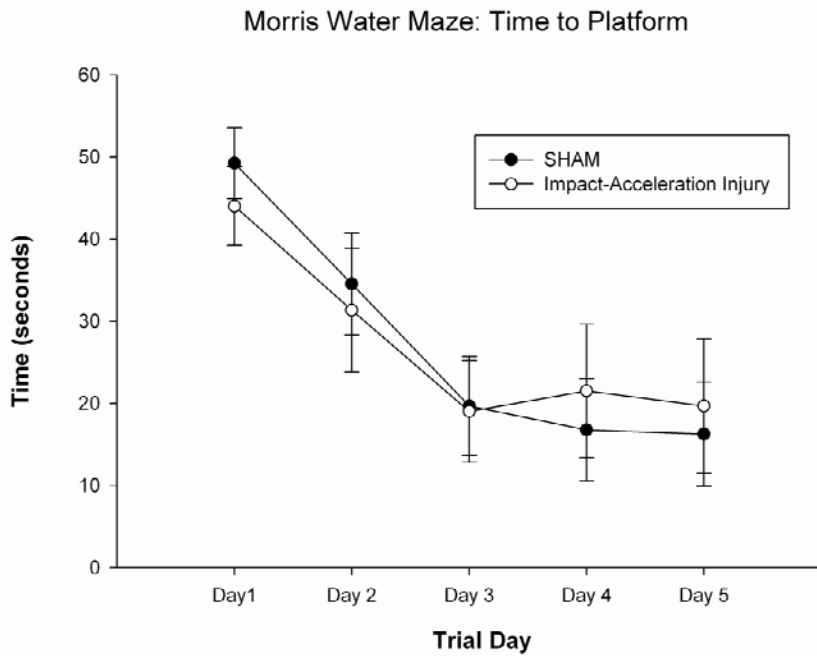


Figure 8: Effect of 0.588 J impact-acceleration injury on learning in the Morris water maze (MWM). Mice were evaluated in MWM on days 5-9 after a 0.588 J impact-acceleration brain injury and the latency to find the hidden platform was evaluated. No significant differences were found between sham and injury groups for any trial day (n=9 per group).

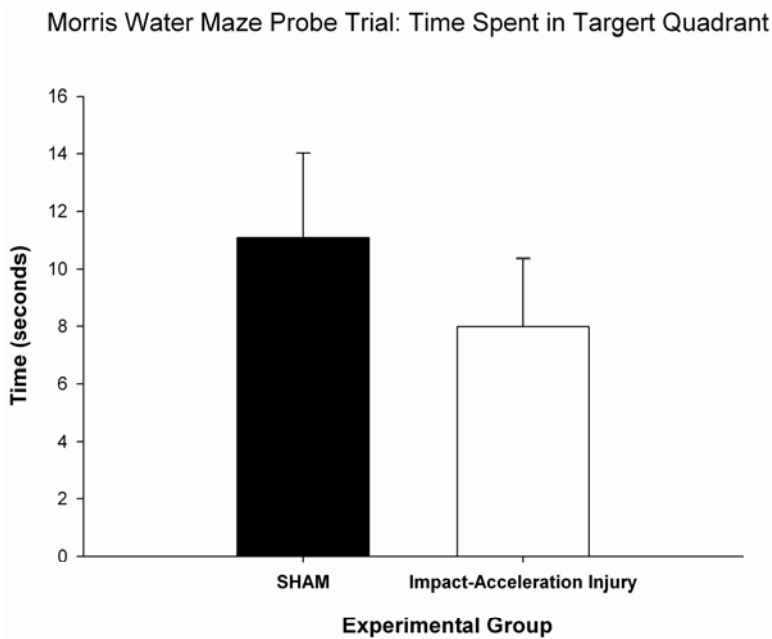


Figure 9: Effect of 0.588 J impact-acceleration brain injury on probe trial in the Morris water maze (MWM). A probe trial was conducted on the last day of MWM evaluation and the time in the target zone was evaluated. There were no significant differences between uninjured (sham) impact-acceleration brain injury group (n=9).

Experimental Group	Average swim speed for learning trials	Average swim speed in probe trial
SHAM	17.8 ± 1.1	21.9 ± 1.7
Impact-Acceleration brain injury	15.1 ± 1.0	20.6 ± 2.5

Table 2: Swim Speed in the Morris water maze for the learning trials (average of trial days 1-5) and the probe trial. No significant differences were found between uninjured control mice (sham group) and mice that received a 0.588 J impact-acceleration brain injury. Values are mean ± standard error of the mean

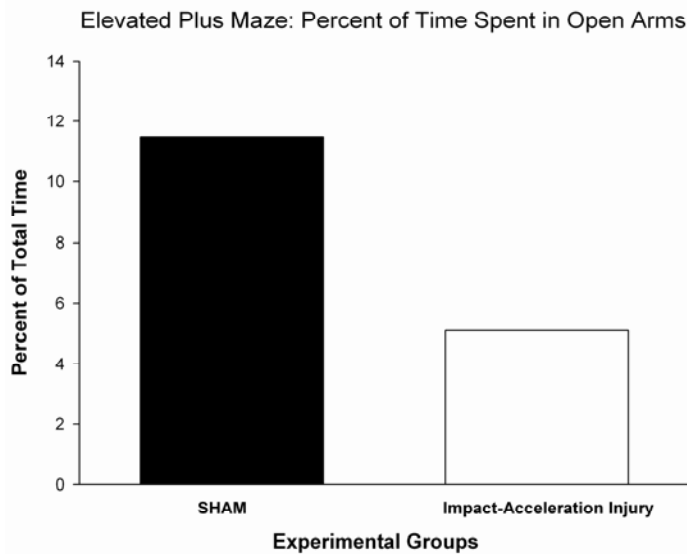


Figure 10: Effect of 0.588J impact-acceleration brain injury on elevated plus maze performance. The elevated plus maze is a behavioral model of anxiety and time spent in open arms in injury versus uninjured (sham) mice was evaluated. Mice that received impact-acceleration brain injury had reduced time in the open arms, suggesting increased anxiety.

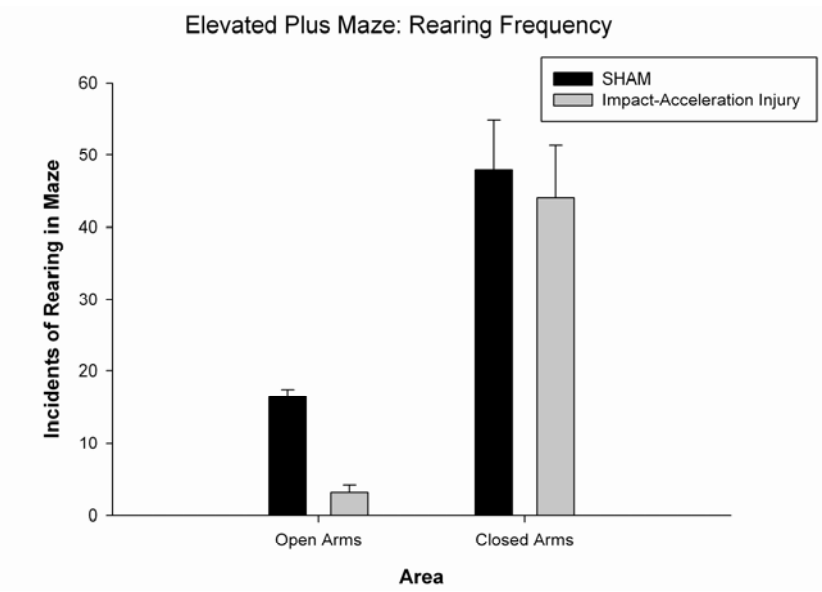


Figure 11: Effect of 0.588J impact-acceleration brain injury on rearing in the elevated plus maze. Rearing is an exploratory behavior that is associated with a lower state anxiety. The number of times an animal reared open versus closed arms was evaluated. Mice that received impact-acceleration brain injury exhibited reduced rearing in the open arms, suggesting increased anxiety.

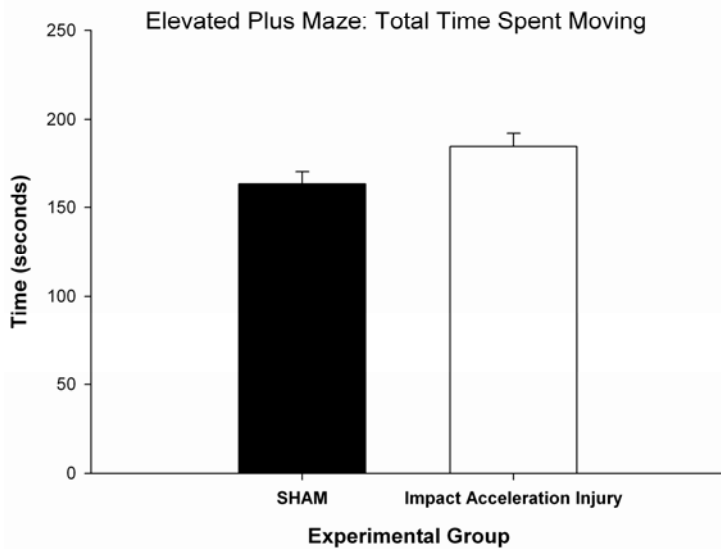
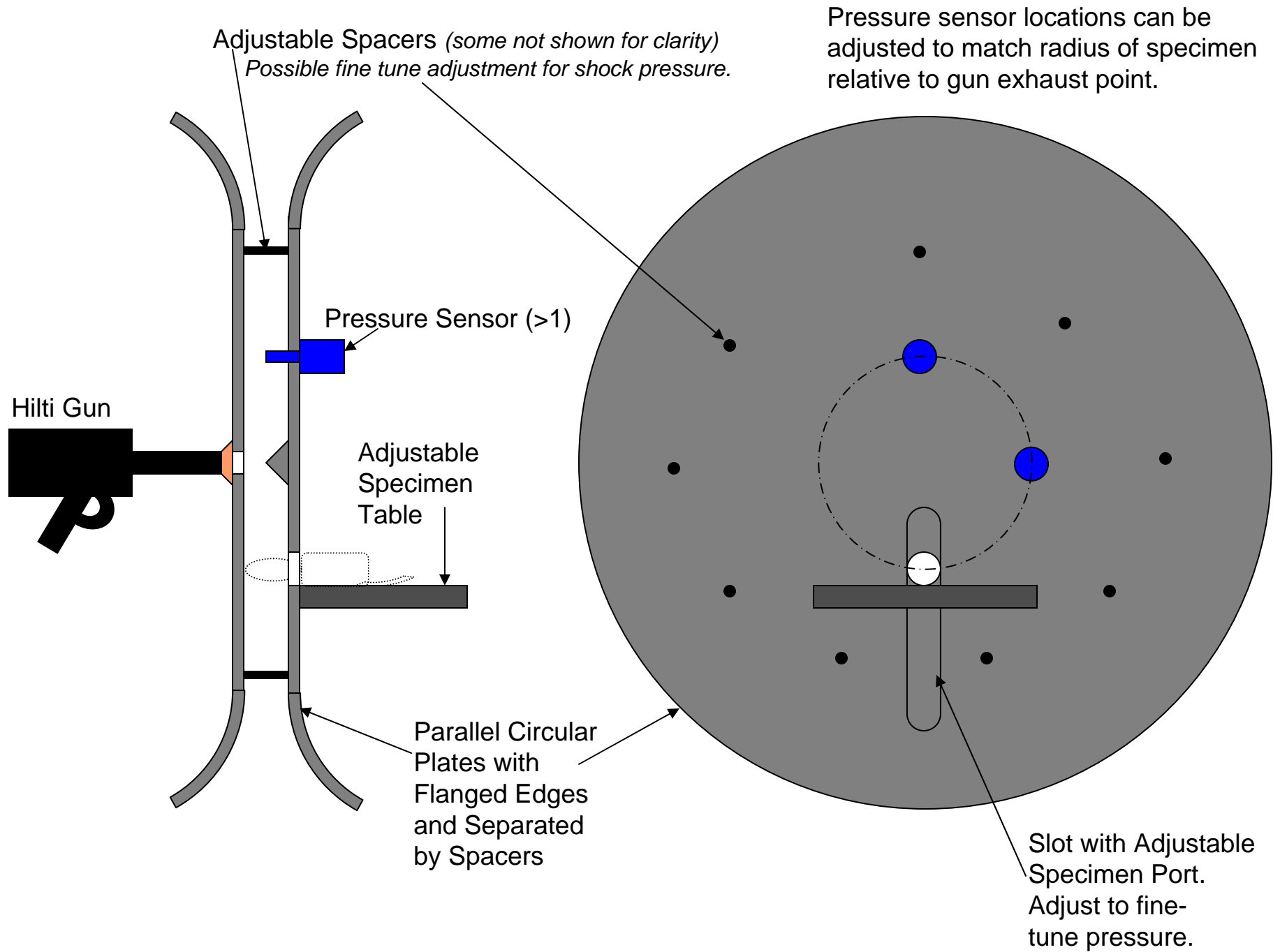


Figure 12: Effect of 0.588J impact-acceleration brain injury on time spent moving in the elevated plus maze. Movement time was evaluated in the elevated plus maze as a measure of motor function. No differences were found between experimental groups, which suggest that motor ability was equal between mice in both groups.



Figure 13: Images from preliminary field test of commercially-available detonation source (0.22 caliber charges in modified Hilti DXE72) into a PVC cylinder (2 inch diameter) of 1 (left panel) or 2 foot length (right panel). The Hilti DXE72 was modified by removing the internal piston.

Figure 14 (next page): Schematic of a new blast chamber design which utilizes a commercially-available detonation source (0.22 caliber charges in modified Hilti DX E72) .



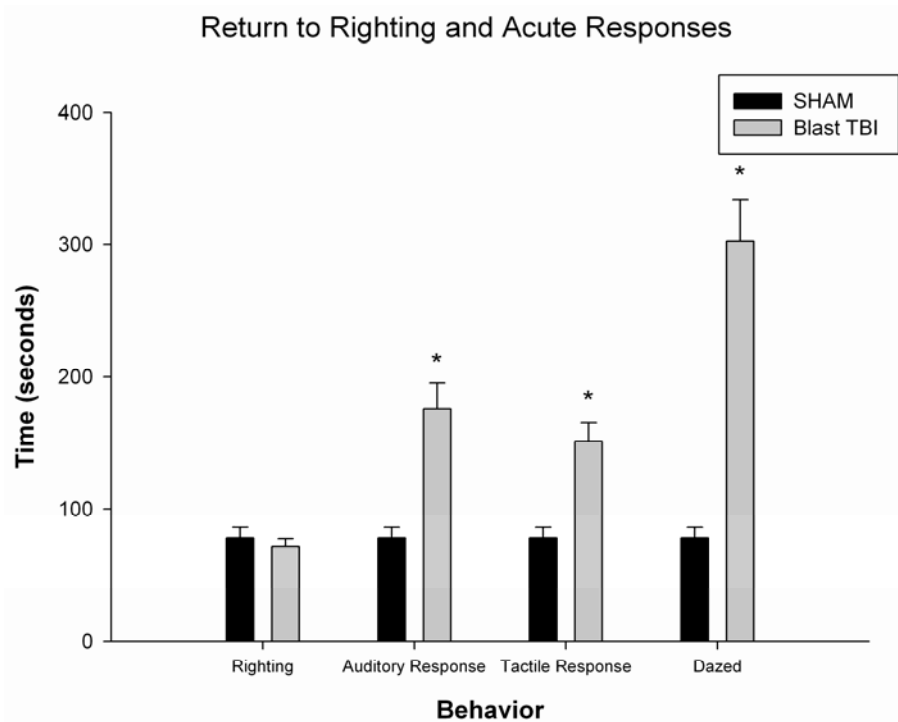


Figure 15: Duration of transient unconscious and altered consciousness following head only blast-exposure. Righting time was not significantly increased in blast-exposed mice as compared to control mice (sham), which suggests that this level of blast-exposure does not induce loss of consciousness. However, blast exposure induced significant acute alterations consciousness as evidenced by significant increases in the duration until auditory response, tactile response and duration of a dazed state in blast-exposed versus control (sham) mice. (n=8-9 per group).

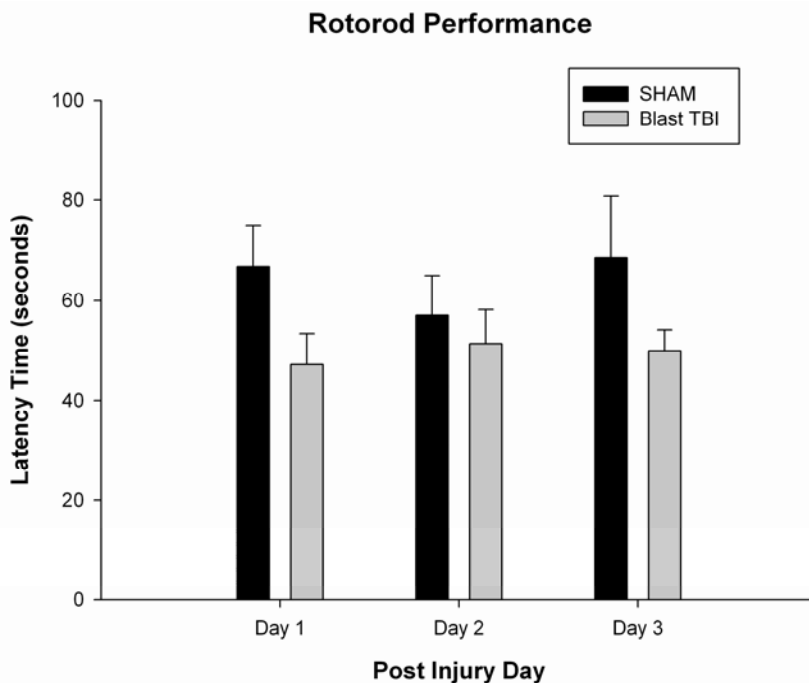


Figure 16: Effect of head only blast-exposure on vestibular motor performance. Mice were trained to balance on an accelerating rod, the Rotorod, and latency to fall off was evaluated on post-blast days 1-3. Blast-exposed mice showed decreased latency on post-blast days 1 and 3. (n=9 per group).

Morris Water Maze: Time to Platform

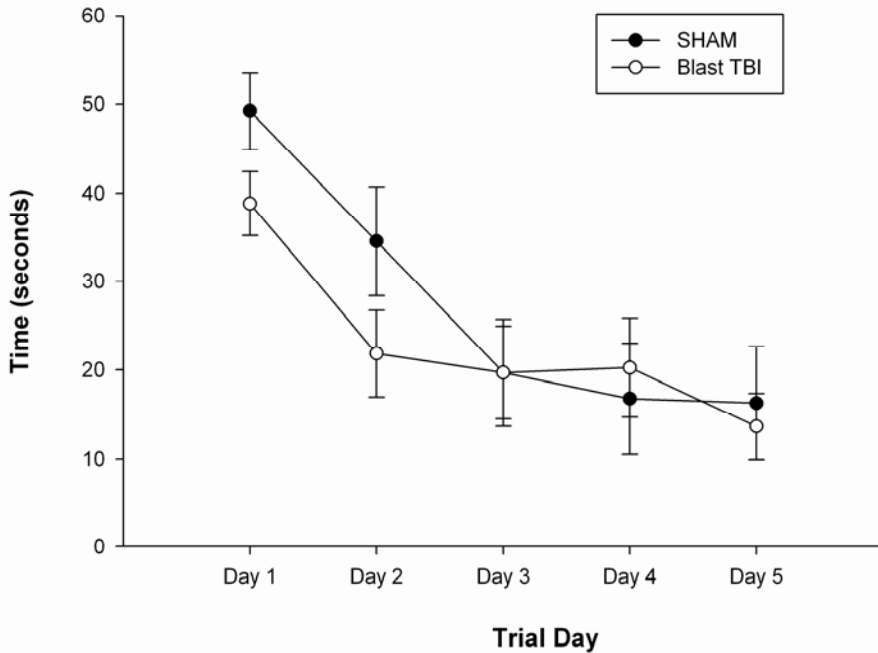


Figure 17: Effect of head only blast-exposure on learning in the Morris water maze (MWM). Mice were evaluated in MWM on days 5-9 after blast-exposure and the latency to find the hidden platform was evaluated. No significant differences were found between sham and injury groups for any trial day (n=9 per group).

Morris Water Maze Probe Trial: Time Spent in Target Quadrant

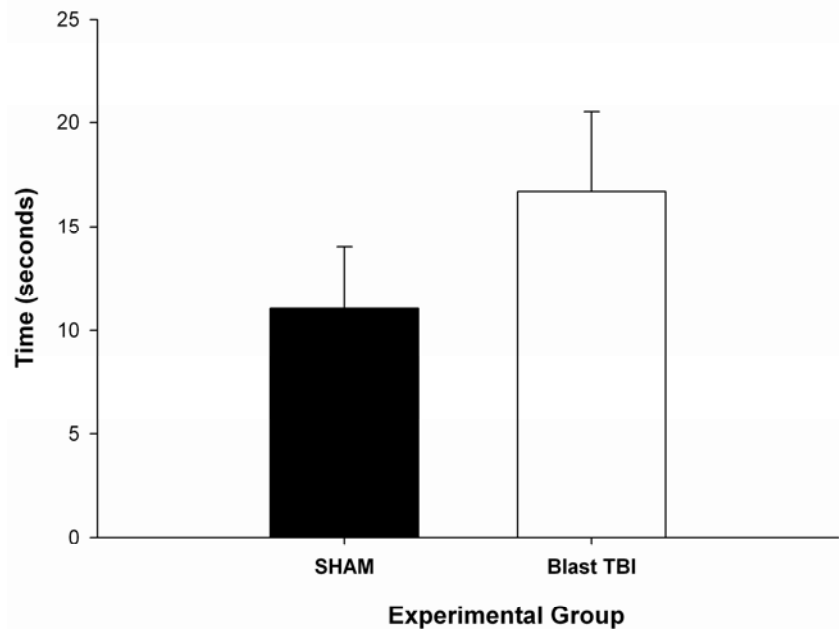


Figure 18: Effect of head only blast-exposure on probe trial in the Morris water maze (MWM). A probe trial was conducted on the last day of MWM evaluation and the time in the target zone was evaluated. There were no significant differences between uninjured (sham) blast-exposed group (n=9 per group).

Experimental Group	Average swim speed for learning trials	Average swim speed in probe trial
SHAM	17.8 ± 1.1	21.9 ± 1.7
Blast-exposed brain injury	14.3 ± 0.8	19.7 ± 1.9

Table 3: Swim Speed in the Morris water maze for the learning trials (average of trial days 1-5) and the probe trial. No significant differences were found between uninjured control mice (sham group) and mice that received head only blast exposure. Values are mean ± standard error of the mean.

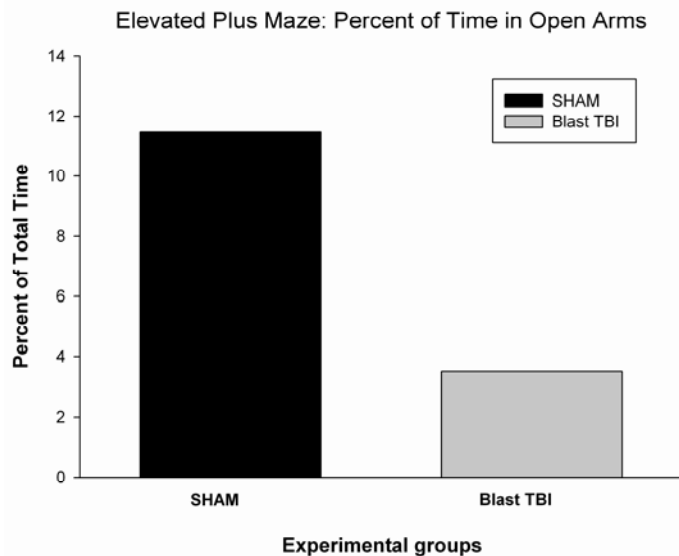


Figure 19: Effect of head only blast exposure on elevated plus maze performance. The elevated plus maze is a behavioral model of anxiety and time spent in open arms in blast-exposed versus uninjured (sham) mice was evaluated. Mice exposed to head only blast exhibited reduced time in the open arms, suggesting increased anxiety. (n=9 per group)

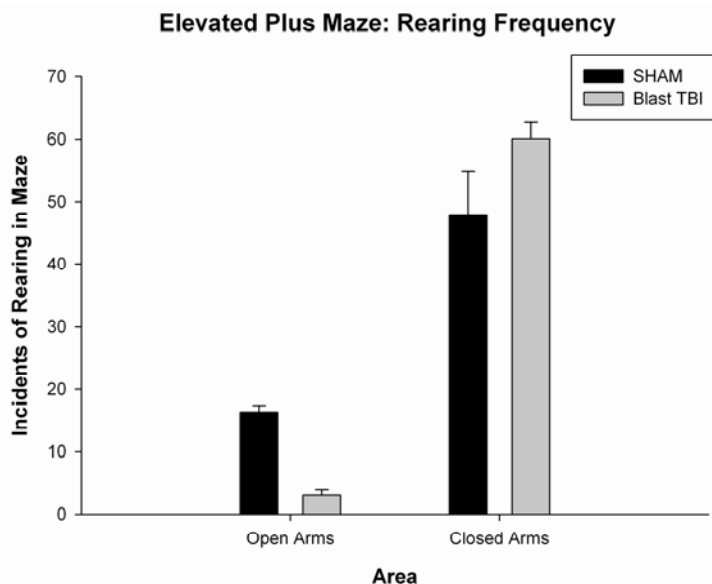


Figure 20: Effect of head only blast exposure on rearing in the elevated plus maze. Rearing is an exploratory behavior that is associated with a lower state anxiety. The number of times an animal reared open versus closed arms was evaluated. Mice that received head only blast exposure exhibited reduced rearing in the open arms, suggesting increased anxiety. (n=9 per group)

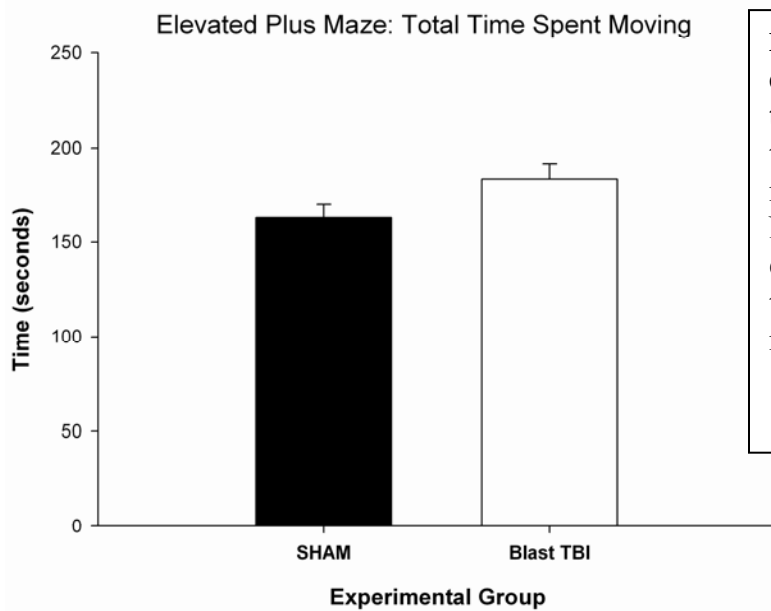


Figure 21: Effect of head only blast exposure on time spent moving in the elevated plus maze. Movement time was evaluated in the elevated plus maze as a measure of motor function. No differences were found between experimental groups, which suggest that motor ability was equal between mice in both groups.

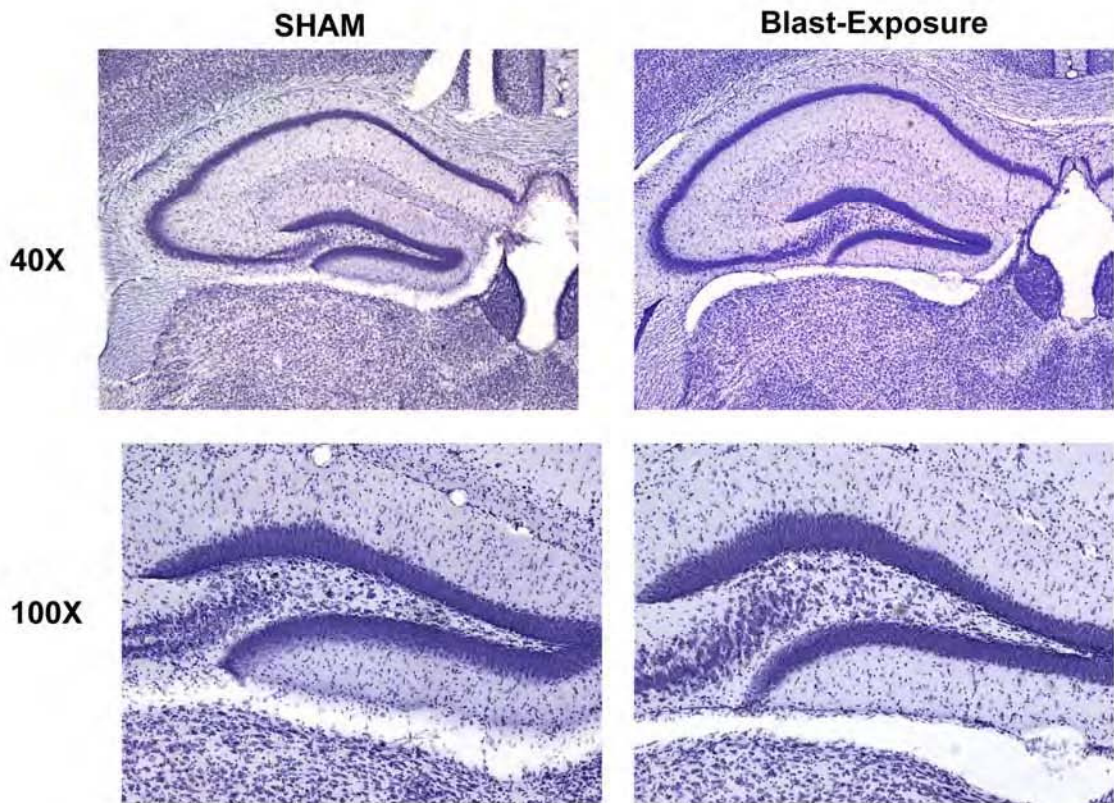


Figure 22: Effect of head only blast-exposure on hippocampal morphology at 48 hours post-exposure. Representative micrographs from serial sections of brain tissue, centering on the hippocampus at 40X (upper) and 100X (lower) magnification. No overt tissue damage was seen in either experimental group.

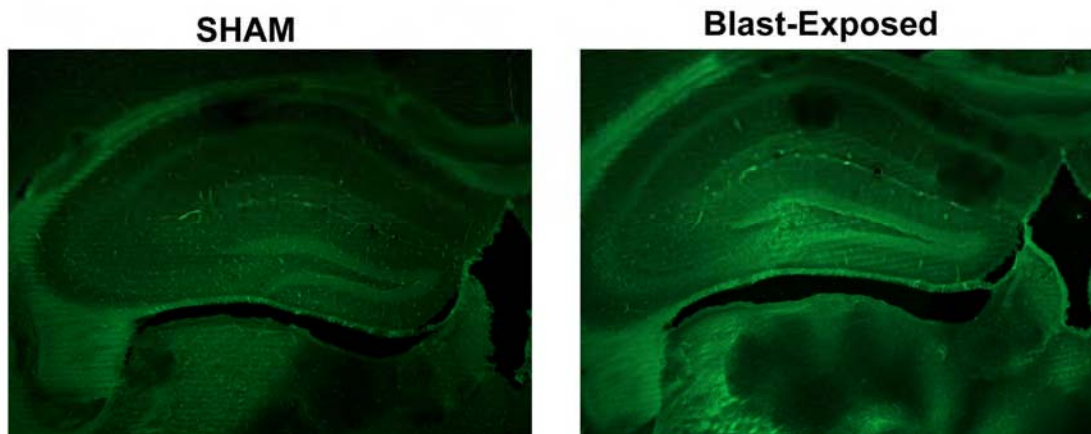


Figure 23: Effect of head only blast-exposure on Fluoro Jade B (FJB) histochemistry in the hippocampus at 48 hours post-exposure. Representative micrographs from serial sections of brain tissue, centering on the hippocampus at 40X. No FJB-positive degenerating neurons were observed.

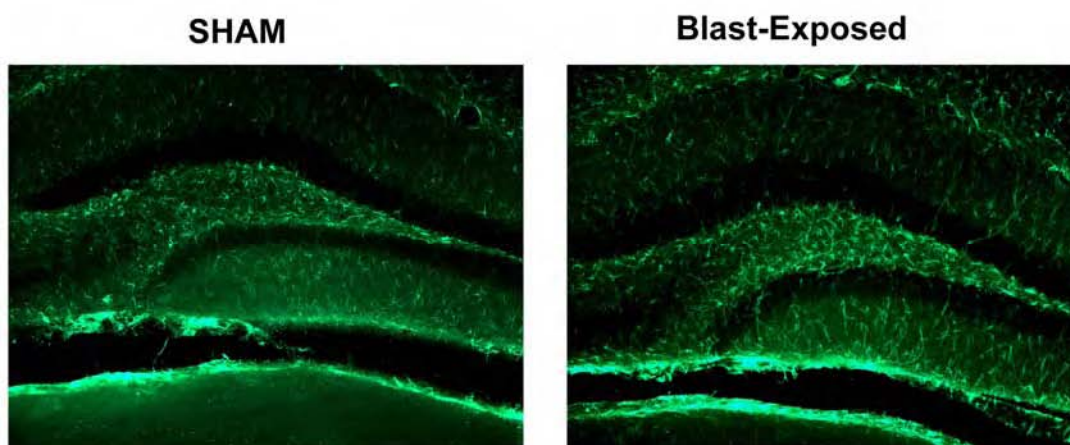


Figure 24: Effect of head only blast-exposure on GFAP immunoreactivity in the hippocampus at 48 hours post-exposure. Representative micrographs from serial sections of brain tissue, centering on the hippocampus at 100X. A slight increase in GFAP immunoreactivity was observed in blast-exposed brain tissue.